



Cite this: *Chem. Commun.*, 2015, 51, 13542

Received 17th June 2015,  
Accepted 16th July 2015

DOI: 10.1039/c5cc05013h

www.rsc.org/chemcomm

# A two-step fluorinase enzyme mediated $^{18}\text{F}$ labelling of an RGD peptide for positron emission tomography†

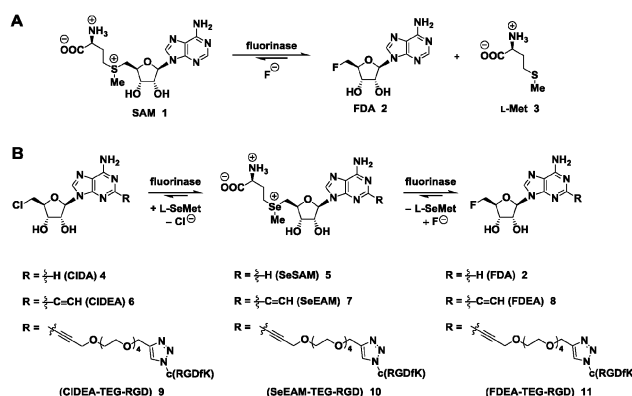
S. Thompson,<sup>a</sup> M. Onega,<sup>b</sup> S. Ashworth,<sup>b</sup> I. N. Fleming,<sup>c</sup> J. Passchier<sup>b</sup> and D. O'Hagan<sup>\*a</sup>

**A two-step radiolabelling protocol of a cancer relevant cRGD peptide is described where the fluorinase enzyme is used to catalyse a transhalogenation reaction to generate  $^{18}\text{F}$ -5'-fluoro-5'-deoxy-2-ethynyladenosine,  $^{18}\text{F}$ FDEA, followed by a 'click' reaction to an azide tethered cRGD peptide. This protocol offers efficient radio-labelling of a biologically relevant peptide construct in water at pH 7.8, 37 °C in 2 hours, which was metabolically stable in rats and retained high affinity for  $\alpha_v\beta_3$  integrin.**

The fluorinase enzyme,<sup>1</sup> involved in the first step of fluorometabolite biosynthesis in a select few bacteria,<sup>2,3</sup> catalyses the reaction of *S*-adenosyl-L-methionine (SAM, 1) and the fluoride ion to generate 5'-fluoro-5'-deoxyadenosine (FDA, 2) and L-methionine (L-Met, 3) (Scheme 1A). The enzyme will also catalyse a transhalogenation reaction when 5'-chloro-5'-deoxyadenosine (ClDA, 4) is presented as a substrate with L-selenomethionine (SeMet) and fluoride.<sup>4</sup> In this case a reverse reaction occurs where SeMet attacks ClDA 4 and generates selenoSAM (SeSAM, 5) *in situ*, after which the fluoride ion, the favoured nucleophile, reacts with SeSAM 5 to generate FDA 2 (Scheme 1B).

Positron emission tomography (PET) has emerged as indispensable functional imaging modality, complementary to anatomical imaging modalities such as magnetic resonance imaging (MRI) and computerised tomography (CT).<sup>5</sup> The development of new methodologies for labelling molecules with positron emitting isotopes (such as carbon-11 and fluorine-18) continues to receive widespread attention, especially for labelling biomolecules.<sup>6</sup>  $^{18}\text{F}$ Fluoride is generated on a cyclotron from  $^{18}\text{O}$ water, and thus in an aqueous form. The most widespread approach for fluorine-18

labelling of biomolecules involves the synthesis of a  $^{18}\text{F}$ -bearing prosthetic group by conventional nucleophilic substitution chemistry using  $^{18}\text{F}$ fluoride, which has been azeotropically dried from  $^{18}\text{O}$ water and formulated in a dry, polar aprotic solvent as the potassium-kryptofix-222 salt.<sup>7</sup> Commonly used prosthetic groups include *N*-succinimide 4- $^{18}\text{F}$ fluorobenzoate ( $^{18}\text{F}$ SFB)<sup>8</sup> and 4- $^{18}\text{F}$ fluorobenzaldehyde ( $^{18}\text{F}$ FBA)<sup>9</sup> for reaction with free amines at the N-terminus or lysine residues of peptides, and maleimides such as 4- $^{18}\text{F}$ fluorobenzaldehyde-*O*-(2-[2-(2-maleimido-*N*-ethoxy)-ethoxy]-ethyl)oxime ( $^{18}\text{F}$ FBOM)<sup>10</sup> for reaction with thiols on cysteine residues. A current challenge is to find aqueous based methods of covalently modifying peptidic ligands with  $^{18}\text{F}$ fluoride to avoid azeotrope drying, such that biomolecules can be rendered readily soluble and be labelled in a reaction in the aqueous phase. The challenge, however, is that fluoride is a very poor nucleophile in water and is difficult to secure. Some good aqueous based methods have been developed recently such as the  $^{18}\text{F}$ AlF methodology<sup>11</sup> where  $^{18}\text{F}$ fluoride is secured by an aluminium-heterocycle complex tethered to a relevant peptide.<sup>12</sup>



**Scheme 1** (A) Native fluorinase-catalysed reaction to give FDA 2 as the first step in fluorometabolite biosynthesis. (B) Fluorinase-catalysed transhalogenation reactions showing SeSAM intermediates, with modified C-2 acetylene-bearing substrates.

<sup>a</sup> School of Chemistry, University of St Andrews, North Haugh, St Andrews, KY16 9ST, UK. E-mail: do1@st-andrews.ac.uk

<sup>b</sup> Imanova, Burlington Danes Building, Imperial College London, Hammersmith Hospital, Du Cane Road, London, W12 0NN, UK

<sup>c</sup> Aberdeen Biomedical Imaging Centre, School of Medicine and Dentistry, University of Aberdeen, Foresterhill, Aberdeen, AB25 2ZD, UK

† Electronic supplementary information (ESI) available: Experimental methods, compound characterisation, LCMS protocols, radiochemistry and imaging protocols. See DOI: 10.1039/c5cc05013h



The fluorinase enzyme functions best in buffer (pH 7.8, 37 °C) under ambient conditions and may present some additional advantages over current methods for this reason. We have recently demonstrated that the C-2 position of the substrate can be substituted with acetylene and this modified substrate, 2-ethynyl-CIDEA (CIDEA, **6**), is processed to 2-ethynyl-FDEA (FDEA, **8**) (~60% rate compared to CIDEA).<sup>13</sup> This led to the demonstration of a 'last step' labelling protocol of a cRGD peptide by extending a tetraethyleneglycol (TEG) chain from the acetylene moiety at C-2 of CIDEA **6** to a cRGD motif to give CIDEA-TEG-RGD **9**, which allowed for the last step fluorinase enzyme based transhalogenation and radiolabelling of this peptide construct with fluorine-18 under ambient conditions (Scheme 1B), generating [<sup>18</sup>F]-FDEA-TEG-RGD [<sup>18</sup>F]-**11**.

In this Communication we demonstrate a complementary two step protocol, both under aqueous, ambient (pH 7.8, 37 °C) conditions, for labelling a cRGD peptide. This involves the transhalogenation of CIDEA (**6**) using [<sup>18</sup>F]fluoride to generate a novel acetylene-bearing radiolabelled prosthetic group, [<sup>18</sup>F]FDEA [<sup>18</sup>F]-**8**, and then coupling the acetylene moiety to an azide bearing cRGD peptide using a copper catalysed 'click' protocol.

We set out to investigate the copper-mediated click reaction under cold conditions, and explore the reaction of both synthetic FDEA (**8**), and that produced by fluorinase transhalogenation with an azide bearing RGD peptide **12**. Firstly, the fluorinase enzyme catalysed transhalogenation of CIDEA **6** (Fig. 1A) was carried out under our previously reported conditions<sup>13</sup> to give a 78:22 mixture of FDEA (**8**,  $t_R$  = 8.5 min) and CIDEA (**6**,  $t_R$  = 10.5 min) in 2 hours (Fig. 1B). After heat precipitation and centrifugation to remove the enzyme, the supernatant containing FDEA **8** (and residual CIDEA **6**) was reacted with c(RGDfK[N<sub>3</sub>]) **12** in the presence of sodium ascorbate and the CuSO<sub>4</sub>-TBTA complex (TBTA = tris[(1-benzyl-1H-1,2,3-triazol-4-yl)methyl]amine)<sup>14</sup> to efficiently generate the triazole, FDEA-RGD (**13**,  $t_R$  = 12.8 min), in 70 minutes (Fig. 1C). The click reaction also proceeded efficiently with synthetic CIDEA **6** and FDEA **8** on a preparative

scale, providing samples of the anticipated products, CIDEA-RGD **14** and FDEA-RGD **13**, for use as reference compounds for the radiolabelling experiments.

The chloromethyl substrate, CIDEA **6**, was then explored in enzymatic radiolabelling experiments using [<sup>18</sup>F]fluoride. Although the reactions progressed at modest conversion in the enzyme assays using [<sup>19</sup>F]fluoride illustrated in Fig. 1, previous experience has shown that fluorinase catalysed radiochemical reactions proceed much faster than assays under cold conditions. The cyclotron generates a solution of [<sup>18</sup>F]fluoride at picomolar concentration, while the fluorinase enzyme is added to this solution at 15–20 mg ml<sup>-1</sup>, which is a micromolar concentration. Therefore there is up to a 10<sup>6</sup> excess of enzyme over fluoride ion concentration in solution. Under these conditions the enzyme is not catalytic, but operates under single turnover conditions. The success of radiochemical experiments lies in converting as much [<sup>18</sup>F]fluoride to organic [<sup>18</sup>F]fluorine as possible and generally very good radiochemical conversions are achieved by fluorinase catalysis with SAM substrates, because of the excess of the enzyme.

In the event [<sup>18</sup>F]FDEA [<sup>18</sup>F]-**8** was produced in 69% radiochemical conversion (RCC). Fig. 2A shows the radiochemical HPLC trace of fluorinase catalysed transhalogenation showing [<sup>18</sup>F]-**8** ( $t_R$  = 7.2 min) as the only radiolabelled product, besides residual [<sup>18</sup>F]fluoride,

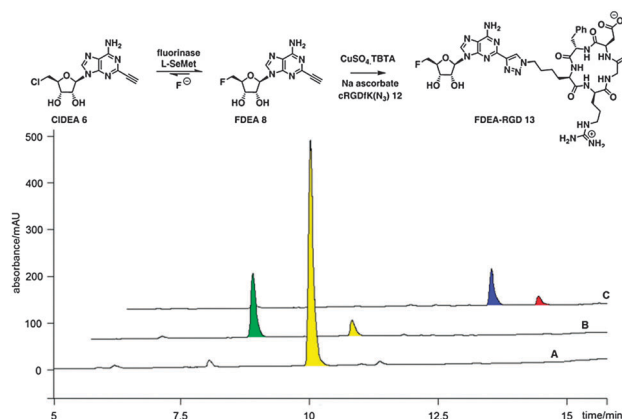


**Fig. 1** (A) Fluorinase-catalysed transhalogenation (pH 7.8, 37 °C) of CIDEA (yellow, **6**) at  $t$  = 0 min. (B) Fluorinase-catalysed transhalogenation of CIDEA (yellow, **6**) to FDEA (green, **8**) at  $t$  = 120 min. (C) Click reaction of enzymatically produced FDEA (**8**, green) with azido-RGD peptide **12** after 70 min showing a new triazole product, FDEA-RGD (**13**, dark blue). CIDEA-RGD (red) is also observed, from residual CIDEA **6** present after transhalogenation.

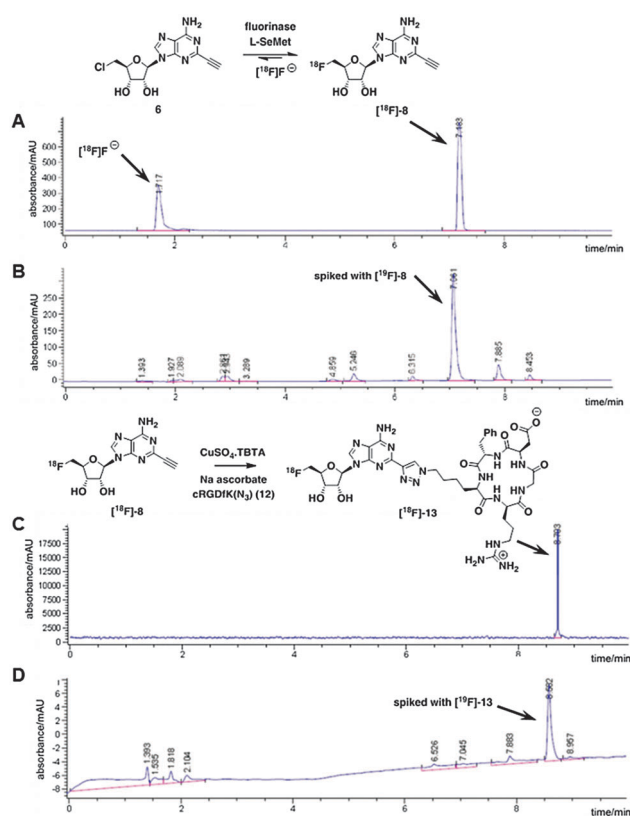


**Fig. 2** (A) Radio-HPLC trace of fluorinase catalysed transhalogenation with [<sup>18</sup>F]fluoride, producing [<sup>18</sup>F]FDEA [<sup>18</sup>F]-**8**. (B) UV-HPLC trace (254 nm) of enzymatically produced [<sup>18</sup>F]FDEA [<sup>18</sup>F]-**8** spiked with a synthetic sample of [<sup>19</sup>F]FDEA **8**. (C) Radio-HPLC trace of purified [<sup>18</sup>F]FDEA-RGD [<sup>18</sup>F]-**13**. (D) UV-HPLC trace (254 nm) of purified [<sup>18</sup>F]FDEA-RGD [<sup>18</sup>F]-**13** spiked with a synthetic sample of [<sup>19</sup>F]FDEA-RGD **13**.



illustrating the high chemoselectivity of the enzymatic radio-fluorination. Spiking with a cold sample of [ $^{19}\text{F}$ ]FDEA **8** confirmed the identity of the radiolabelled product (Fig. 2B).

The click reaction of [ $^{18}\text{F}$ ]FDEA [ $^{18}\text{F}$ ]-**8** with azido-RGD peptide (**12**) was found to be complete within 30 minutes generating [ $^{18}\text{F}$ ]FDEA-RGD ([ $^{18}\text{F}$ ]-**13**,  $t_R = 8.7$  min) quantitatively. [ $^{18}\text{F}$ ]-**13** was then purified by reverse phase semi-preparative HPLC and reformulated into 10% ethanol in saline to give a dose suitable for an animal study (Fig. 2C). Total synthesis time was 2 hours and produced [ $^{18}\text{F}$ ]FDEA in up to 20% non-decay corrected radiochemical yield. Spiking with a cold sample of [ $^{19}\text{F}$ ]FDEA-RGD confirmed the identity of the new product (Fig. 2D).

There is some uncertainty as to the metabolic stability of these C-2 substituted adenosine analogues. If such compounds are metabolised, such that fluoride ion is released, then they become redundant as PET radiotracers because the released [ $^{18}\text{F}$ ]fluoride accumulates in the bone.<sup>15</sup> This issue was addressed satisfactorily in the last step labelling study reported recently,<sup>13</sup> where the radiolabelled product was injected into healthy rats to evaluate defluorination and bone uptake. The radiolabelled product in that study, [ $^{18}\text{F}$ ]FDEA-TEG-RGD, [ $^{18}\text{F}$ ]-**11** (Scheme 1B), proved to be metabolically stable to [ $^{18}\text{F}$ ]fluoride release showing no enhanced bone uptake, and normal urinary clearance.

We have carried out a similar study for [ $^{18}\text{F}$ ]-**13** by injecting two male Sprague-Dawley rats with a radiotracer. One rat was imaged by PET-CT, and blood samples from both rats were monitored to assess the metabolism of [ $^{18}\text{F}$ ]-**13**. The summed PET-CT of the imaged rat showed negligible uptake of activity in bone. Acetonitrile extracts of blood plasma samples taken at various intervals (5, 15, 30 and 60 minutes post injection) from both rats all showed a single radioactive compound present in the reconstructed HPLC-radiochromatogram and negligible [ $^{18}\text{F}$ ]fluoride ion release. This was confirmed to be [ $^{18}\text{F}$ ]-**13** by co-injection with [ $^{19}\text{F}$ ]-**13**, showing the stability of the construct to metabolic processing.

The biodistribution of [ $^{18}\text{F}$ ]-**13** in the PET-CT images was similar to the natural biodistribution of  $\alpha_v\beta_3$ , locating primarily in the liver and intestinal wall, as well as the kidneys and bladder (see Fig. 3 and Fig. S19, ESI†).<sup>16</sup>

Evaluating the binding of test molecules to immobilised  $\alpha_v\beta_3$  integrin is a standard method of assessing binding affinities of RGD peptides.<sup>17</sup> The affinity of the peptide for  $\alpha_v\beta_3$  is measured as  $\text{IC}_{50}$ , but normalized to the  $\text{IC}_{50}$  of a reference peptide (GRGDSPK) to allow inter-assay comparisons. The normalized affinity, "Q", is defined as  $\text{IC}_{50}(\text{peptide})/\text{IC}_{50}(\text{GRGDSPK})$  by Haubner *et al.*<sup>17</sup> Affinity of RGD, GRGDSPK, c(RGDfK[N<sub>3</sub>]) **12**, and FDEA-RGD **8** for immobilised  $\alpha_v\beta_3$  integrin was measured against c(RGDfK[PEG-PEG-biotin]) in a competition-based assay. The  $\text{IC}_{50}$  value of **8** was found to be  $0.33 \pm 0.03 \mu\text{M}$  with a Q factor of 0.155 (Table 1). FDEA-RGD **8** retains the well-documented<sup>18</sup> order of magnitude with greater affinity for  $\alpha_v\beta_3$  integrin compared to the linear reference peptides in this assay *e.g.* RGD at  $8.56 \pm 2.24 \mu\text{M}$ /Q = 4.02. The  $\text{IC}_{50}$  was the same order of magnitude as unmodified c(RGDfK[N<sub>3</sub>]) **12**, which had an  $\text{IC}_{50}$  of  $0.09 \pm 0.005 \mu\text{M}$ . The Q factor for FDEA-RGD **8** compares moderately well to other well-characterised high affinity  $\alpha_v\beta_3$  ligands, such

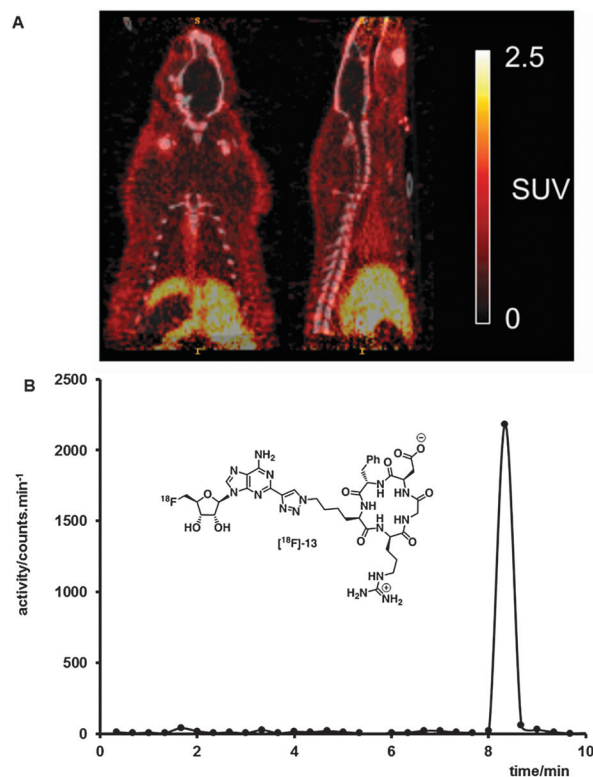


Fig. 3 (A) Sagittal and coronal summed PET-CT images (0–70 min) with the head and thorax in the field of view (FOV) showing the accumulation of [ $^{18}\text{F}$ ]-**13** in the liver. The CT image in the grayscale, PET in colour. PET images are presented as standard uptake values ( $\text{SUV} = \{(\text{tissue activity}/\text{mL})/(\text{injected activity}/\text{animal weight}[\text{g}])\}$ ). Tracer uptake in the bone is negligible, indicating that the construct is stable to defluorination. (B) Reconstructed radio-HPLC chromatogram of acetonitrile extracts of plasma after 60 min showed only [ $^{18}\text{F}$ ]FDEA-RGD [ $^{18}\text{F}$ ]-**13** present in the plasma.

Table 1  $\text{IC}_{50}$  values of RGD-containing peptide motifs measured as the ability of the peptide to compete with c(RGDfK[PEG-PEG-biotin]) for binding to immobilised  $\alpha_v\beta_3$  integrin. RGD and GRGDSPK are used as reference peptides. Results are the average  $\pm$  standard error (s.e.) from three independent experiments performed in triplicate. Q is the normalised activity of the peptides, referenced to GRGDSPK

Compound	$\text{IC}_{50} \pm \text{s.e.}/\mu\text{M}$	Q
RGD <sup>a</sup>	$8.56 \pm 2.24$	4.019
GRGDSPK (Ref. peptide) <sup>a</sup>	$2.13 \pm 0.41$	1.000
c(RGDfK[N <sub>3</sub> ]) <b>12</b>	$0.09 \pm 0.005$	0.042
FDEA-RGD <b>13</b>	$0.33 \pm 0.03$	0.155

<sup>a</sup> The  $\text{IC}_{50}$  values for these compounds were reported previously,<sup>19</sup> and measured in an identical assay.

as c(RGDfV) whose Q factor has been reported to be 0.033.<sup>19</sup> These data show that the fluorodeoxyadenosine moiety does not significantly perturb the binding of the cRGD motif to  $\alpha_v\beta_3$  integrin.

In conclusion, we demonstrate a straightforward two-step radiolabelling protocol for cRGD peptides. This method complements our recently disclosed 'last step' radiolabelling protocol and despite the extra step, it has some advantage in that the enzyme substrate, CIDEA **6**, is more readily prepared synthetically. Normally fluorine-18 labelling protocols require



[ $^{18}\text{F}$ ]-fluoride in dry, non-aqueous solvent. This method takes place in aqueous buffer (pH 7.8) at 37 °C. The optimal ligands for tumour imaging have to await the outcomes of *in vivo* studies in different animal tumour models.

We thank EPSRC and the Scottish Imaging Network (SINAPSE) for grants. DO'H thanks the Royal Society for a Wolfson Research Merit Award and ST is grateful to the John and Kathleen Watson Scholarship for financial support.

## Notes and references

- 1 D. O'Hagan, C. Schaffrath, S. L. Cobb and J. T. G. Hamilton, *Nature*, 2002, **416**, 289.
- 2 H. Deng, L. Ma, N. Bandaranayaka, Z. Qin, G. Mann, K. Kyeremeh, Y. Yu, T. Shepherd, J. H. Naismith and D. O'Hagan, *ChemBioChem*, 2014, **15**, 364–368.
- 3 S. Huang, L. Ma, M. H. Tong, Y. Yu, D. O'Hagan and H. Deng, *Org. Biomol. Chem.*, 2014, **12**, 4828–4831.
- 4 H. Deng, S. L. Cobb, A. R. McEwan, R. P. McGlinchey, J. H. Naismith, D. O'Hagan, D. A. Robinson and J. B. Spencer, *Angew. Chem., Int. Ed.*, 2006, **45**, 759–762.
- 5 O. Mawlawi and D. W. Townsend, *Eur. J. Nucl. Med. Mol. Imaging*, 2009, **36**, 15–29.
- 6 V. Tolmachev and S. Stone-Elander, *Biochim. Biophys. Acta*, 2010, **1800**, 487–510.
- 7 L. Cai, S. Lu and V. W. Pike, *Eur. J. Org. Chem.*, 2008, 2853–2873.
- 8 G. Vaidyanathan and M. R. Zalutsky, *Nat. Protoc.*, 2006, **1**, 1655–1661.
- 9 Y. S. Chang, J. M. Jeong, Y.-S. Lee, H. W. Kim, G. B. Rai, S. J. Lee, D. S. Lee, J.-K. Chung and M. C. Lee, *Bioconjugate Chem.*, 2005, **16**, 1329–1333.
- 10 F. Wuest, L. Köhler, M. Berndt and J. Pietzsch, *Amino Acids*, 2009, **36**, 283–295.
- 11 (a) W. J. McBride, C. A. D'Souza, R. M. Sharkey and D. M. Goldenberg, *Appl. Radiat. Isot.*, 2012, **70**, 200–204; (b) W. J. McBride, C. A. D'Souza, R. M. Sharkey, H. Karacay, E. A. Rossi, C. H. Chang and D. M. Goldenberg, *Bioconjugate Chem.*, 2010, **21**, 1331–1340; (c) S. Liu, H. Liu, H. Jiang, Y. Xu, H. Zhang and Z. Cheng, *Eur. J. Nucl. Med. Mol. Imaging*, 2011, **38**, 1732–1741.
- 12 W. Wan, N. Guo, D. Pan, C. Yu, Y. Weng, S. Luo, H. Ding, Y. Xu, L. Wang, L. Lang, Q. Xie, M. Yang and X. Chen, *J. Nucl. Med.*, 2013, **54**, 691–698.
- 13 S. Thompson, Q. Zhang, M. Onega, S. McMahon, I. Fleming, S. Ashworth, J. H. Naismith, J. Passchier and D. O'Hagan, *Angew. Chem., Int. Ed.*, 2014, **53**, 8913–8918.
- 14 R. Chan, R. Hilgraf, K. B. Sharpless and V. V. Fokin, *Org. Lett.*, 2004, **6**, 2853–2855.
- 15 V. W. Pike, *Trends Pharmacol. Sci.*, 2009, **30**, 431–440.
- 16 J. Oxboel, M. Brandt-Larsen, C. Schjoeth-Eskesen, R. Myszchetsky, H. H. El-Ali, J. Madsen and A. Kjaer, *Nucl. Med. Biol.*, 2014, **41**, 259–267.
- 17 R. Haubner, H.-J. Wester, U. Reuning, R. Senekowitsch-Schmidtke, B. Diefenbach, H. Kessler, G. Stöcklin and M. Schwaiger, *J. Nucl. Med.*, 1999, **40**, 1061–1071.
- 18 R. Haubner, R. Gratias, B. Diefenbach and S. Goodman, *J. Am. Chem. Soc.*, 1996, **118**, 7461–7472.
- 19 M. Piras, I. Fleming, W. Harrison and M. Zanda, *Synlett*, 2012, 2899–2902.

